

Solar Spectral Irradiance Variability in November/December 2012: Comparison of Observations by Instruments on the *International Space Station* and Models

G. Thuillier · G. Schmidtke · C. Erhardt · B. Nikutowski · A.I. Shapiro · C. Bolduc ·
J. Lean · N. Krivova · P. Charbonneau · G. Cessateur · M. Haberreiter · S. Melo ·
V. Delouille · B. Mampaey · K.L. Yeo · W. Schmutz

Received: 24 April 2014 / Accepted: 30 July 2014 / Published online: 22 August 2014
© Springer Science+Business Media Dordrecht 2014

Abstract Onboard the *International Space Station* (ISS), two instruments are observing the solar spectral irradiance (SSI) at wavelengths from 16 to 2900 nm. Although the ISS platform orientation generally precludes pointing at the Sun more than 10–14 days *per* month,

G. Thuillier (✉)
LATMOS-CNRS, 11 Blvd d'Alembert, 78280 Guyancourt, France
e-mail: gerard.thuillier@latmos.ipsl.fr

G. Schmidtke · C. Erhardt · B. Nikutowski
Fraunhofer Institute for Physical Measurement Techniques, Heidenhofstrasse 8, 79110 Freiburg,
Germany

B. Nikutowski
Institute for Meteorology, University of Leipzig, Stephanstr. 3, 04103 Leipzig, Germany

A.I. Shapiro · G. Cessateur · M. Haberreiter · W. Schmutz
Physikalisch-Meteorologisches Observatorium Davos, World Radiation Center, 7260 Davos Dorf,
Switzerland

C. Bolduc · P. Charbonneau
Département de Physique, Université de Montréal, C.P. 6128, Montréal, QC, H2C 3J7, Canada

J. Lean
Space Science Division, Naval Research Laboratory, 4555 Overlook Ave. SW, Washington, DC 20375,
USA

N. Krivova · K.L. Yeo
Max-Planck-Institute für Sonnensystemforschung, Göttingen, Germany

S. Melo
Department of Physics, University of Toronto, 50 George St, Toronto, Ontario, Canada

V. Delouille · B. Mampaey
Solar-Terrestrial Centre of Excellence, Brussels, Belgium

V. Delouille · B. Mampaey
Royal Observatory of Belgium, Brussels, Belgium

in November/December 2012 a continuous period of measurements was obtained by implementing an ISS ‘bridging’ maneuver. This enabled observations to be made of the solar spectral irradiance (SSI) during a complete solar rotation. We present these measurements, which quantify the impact of active regions on SSI, and compare them with data simultaneously gathered from other platforms, and with models of spectral irradiance variability. Our analysis demonstrates that the instruments onboard the ISS have the capability to measure SSI variations consistent with other instruments in space. A comparison among all available SSI measurements during November–December 2012 in absolute units with reconstructions using solar proxies and observed solar activity features is presented and discussed in terms of accuracy.

Keywords Spectral solar irradiance variability · International Space Station · SOLSPEC · SolACES · Solar Modeling

1. Introduction and Scientific Motivation

The long-term variability of the solar spectral irradiance (SSI) exhibits approximate periodicities at 27 days and 11 years, with wavelength-dependent amplitudes traceable to the origins of the emission within different layers of the solar atmosphere. The primary cause of SSI variability is the occurrence of active regions in the solar atmosphere, and the balance between the darkening by sunspots and pores and the enhanced brightness of the faculae and network. In general, solar variability increases in amplitude with decreasing wavelengths, as concerned species emit photons at higher altitude in the solar atmosphere.

The Sun’s rotation, which transports active regions across the solar hemisphere visible from the Earth, induces SSI variability with a period near 27 (and sometimes 13) days. The temporal structure of this rotation modulation of solar irradiance depends on the patterns of emergence, evolution, and decay of the active regions. This variability is indirectly linked to the 11-year solar activity cycle in that high solar activity increases the number of active regions and hence the overall amplitude of the 27-day irradiance modulation. Studying the amplitude of SSI variability as a function of wavelength during solar rotation is important for:

- Solar physics, because it demonstrates the relationship of the changing locations and extent of active regions with solar irradiance. Such information is required for the validation of empirical and theoretical models of the solar atmosphere.
- Planetary atmospheres, which have specific properties (composition and temperature) that generally vary in phase with the Sun’s rotation,
- Models of the Earth’s atmosphere, which use the 27-day variability to test their capability in comparison with measurements of, for example, ozone concentration variations.

Consequently, reliable and validated measurements of the SSI from space are key parameters for understanding the physics of the Sun, climate, and planetary atmospheres. Continuous time series are crucial because individual solar cycles evolve differently in length and amplitude. Cycle 24, for example, commenced after an unexpected prolonged minimum during 2008–2009, and is relatively weak, compared to the three previous cycles 21, 22, and 23.

An international effort to precisely measure and understand solar spectral irradiance variability has been under way for some decades, with measurements made by different instruments on a variety of space platforms, including the *Solar Backscatter UltraViolet*

(SBUV) instruments onboard National Aeronautical Space Administration (NASA) and National Oceanic and Atmospheric Administration (NOAA) spacecraft (Cebula *et al.*, 1992), the *Solar Ultraviolet Spectral Irradiance Monitor* (SUSIM, Brueckner *et al.*, 1993) and *SOLar STEllar Irradiance Comparison Experiment* (SOLSTICE, Rottman *et al.*, 1993) onboard the *Upper Atmosphere Research Satellite* (UARS), and *SOLar SPECtrum* (SOLSPEC, Thuillier *et al.*, 2009) flown on three *Atmospheric Laboratory for Applications and Science* (ATLAS) missions. Whereas the SBUV, SUSIM, and SOLTICE instruments observed only the ultraviolet solar spectrum (100 to 400 nm), SOLSPEC made the first direct space-based measurements of the spectral irradiance simultaneously at ultraviolet, visible, and infrared wavelengths. These several decades of space spectrophotometry observations indicate that degradation of the instrument's sensitivity is the primary difficulty limiting the accuracy and repeatability of observations of solar spectral irradiance and its variability, at all wavelengths. Many efforts, based on the use of internal calibration lamps, ionization chambers (IC), stable-star irradiance references, optical redundancy and twin-instrument inter-comparisons, and twin-instrument rocket flights, were made with the goal of maintaining the absolute photometric scale of solar spectrophotometers for the duration of their space-based missions.

Since 2002, a new generation of instruments is measuring the entire solar spectrum from the extreme ultraviolet (EUV) spectrum to the near infrared. The *SCanning Imaging Absorption spectrometer for Atmospheric CHartograpY* (SCIAMACHY, Bovensmann *et al.*, 1999), SOLSTICE (McClintock *et al.*, 2005) and *Spectral Irradiance Monitor* (SIM, Harder *et al.*, 2010) on the *Solar Radiation and Climate Experiment* (SORCE, Rottman, 2005), *SOLar SPECtrum* (SOLSPEC, Thuillier *et al.*, 2009, 2013b) and *Solar Auto Calibrating EUV/UV Spectrometers* (SolACES, Schmidtke *et al.*, 2006a), which constitute the SOLAR (Schmidtke *et al.*, 2006b) payload onboard the ISS, use a variety of onboard and under-flight calibration techniques to monitor in-flight instrument sensitivity changes. These advances have significantly improved the specification of varying solar EUV irradiance such that data from the *Thermosphere Ionosphere Mesosphere Energetics and Dynamics* (TIMED, Woods *et al.*, 2005), *Solar Heliospheric Observatory* (SoHO), *Project for OnBoard Autonomy* (PROBA-2, Dominique *et al.*, 2013), SOLAR, and *Extreme Ultraviolet Variability Experiment* (EVE, Woods *et al.*, 2012), *Solar Dynamics Observatory* (SDO) provide the most reliable, thus far, estimates of the magnitude of irradiance variability, not just during solar rotational modulation, but also on the longer time scales of the solar cycle. But while the accuracy of the near ultraviolet – visible spectral irradiance has improved, uncertainties remain about the magnitude of variability reported by SIM on SORCE at the end of cycle 23, which differs notably from prior UARS observations and models of solar spectral irradiance variability that account for the active region influences (Haigh *et al.*, 2010; Thuillier *et al.*, 2012) possible because of unresolved sensitivity changes in the SIM (Lean and DeLand, 2012).

A reliable attribution of global change in the Earth's atmosphere and in surface climate requires knowledge of natural variability induced by changing solar irradiance and volcanic aerosols, in addition to anthropogenic greenhouse gas concentrations. In particular, because the Earth's atmosphere absorbs solar spectral irradiance over a wide range of altitudes, state-of-the-art climate model simulations now require the input of the entire solar spectrum and its variability (Schmidt *et al.*, 2011), not of just the total (spectrally integrated) solar irradiance (TSI). In particular, changes in ozone concentrations and stratospheric radiation, chemistry, and dynamics in the response to changing solar ultraviolet irradiance are invoked to explain the amplitude of the observed temperature variations on decadal to century time scales, involving amplification by dynamical coupling between the stratosphere and troposphere (*e.g.* Meehl *et al.*, 2009; Anet *et al.*, 2013).

For estimating SSI at times preceding the space-age measurements, for use in global change simulations, models have been developed to estimate irradiance changes arising from sunspot and facular influences, using various proxies of solar activity that exist over multiple decades. The models' estimates of contemporary irradiance spectra with available direct observations anchor and validate these historical reconstructions. Furthermore, the reconstructions allow for interpolation between data interruptions and may assist in identifying instrument sensitivity changes (*e.g.* Lean and DeLand, 2012). However, various irradiance reconstructions may themselves disagree (in different ways at different wavelengths) depending on the solar activity proxies used, the assumptions made to connect solar activity and irradiance, and the accuracy and the property of the proxies. Recent comparisons of solar spectral irradiance variability models that focused primarily on the long-term reconstructions shows general overall agreement but also some significant differences at certain periods, especially at low solar activity, and in the UV spectral regions (Thuillier *et al.*, 2013a).

Long-term solar variability specification requires extremely stable instruments, with no aging or very precise corrections for on-orbit sensitivity changes, both of which have proven difficult to achieve. However, short-term variability studies can be undertaken by observing a single solar rotation, which generates an irradiance change (*e.g.* maximum to minimum), induced by the active regions' movement in the field of view of the instrument. To correctly capture such irradiance variability, it is crucial to make observations that cover a full solar rotation. Since the SolACES and SOLSPEC measurements are periodically interrupted due to the ISS orbital attitude and the limitation of the solar pointing platform capability on which these two instruments are mounted, normal operations do not allow for the possibility of covering a full solar rotation. Using fractions of the solar rotation period rather than a full solar rotation strongly limits the accuracy of the study of active region effects. For this reason, a change of the nominal attitude of ISS was requested and approved, with the Space Agencies strongly supporting a special operation. The measurements were made in November/December 2012, and enabled the following studies:

- Verification by cross-comparison the ability of all existing instruments to reliably measure the amplitude of the EUV and UV solar irradiance variability.
- Models validation of the sunspots and faculae effects on the UV irradiance.
- Utilization of models based on solar proxies to reconstruct the solar spectrum for comparison with the SOLAR observations.
- Verification of the method of extracting EUV spectra from modeled ionization chamber measurements of SolACES.
- Verification of the method of deriving the integrated SSI shorter than 17 nm from background currents of the SolACES ionization chambers.

The variation of the EUV and UV solar irradiance spectrum has important effects on the Earth's atmosphere, *i.e.* on its temperature, density, composition, and dynamics. In order to determine these effects with high accuracy it is important to have a continuous time series with a complete wavelength coverage. However, as observations in this spectral range are inhomogeneous in time, modeling the EUV–UV variability in a robust way is an important step in advancing our understanding of their effects on the Earth's atmosphere. This is why the approach used in this paper follows Thuillier *et al.* (2013a), except that here we concentrate on the shorter-timescale variability induced by the solar rotation, in the spectral range spanning the EUV to the UV.

2. Instrumentation Descriptions

On the ISS SOLAR platform, two instruments participated in the November/December 2012 campaign, namely SolACES and SOLSPEC, especially activated during this period. They are briefly described below.

2.1. SolACES

SolACES (Schmidtke *et al.*, 2006a, 2014) records the solar EUV irradiance from 16 nm to 150 nm with a wavelength-dependent spectral resolution of 0.5 nm to 1.8 nm. The instrument uses three grazing incidence planar grating spectrometers. On the optical entrances of two three-signal double-ionization chambers (IC), a filter wheel inserts a series of band-pass filters. The filter transmission is repeatedly measured by the spectrometers. The current generated by the absorption of the transmitted EUV photons into the ionization chambers is the measure of the absolute photon fluxes. Ionization chambers are considered as a primary detector standard at those wavelengths for which one EUV photon produces one ion-electron pair. For each of these calibration measurements, the ionization chambers are refilled with gas. SolACES is operated up to several times *per* day in order to capture the high variability of the EUV solar spectral irradiance, which this instrument observes. The design of SolACES allows long-term studies. The absorption cross-sections of the idle gases being constant, the ionization chambers are primary calibration standards, providing that the changes of the filter transmission can be determined, which is performed with SolACES. Furthermore, the NIST electron synchrotron radiation has been validated via ionization chambers in the XUV spectral range, which includes EUV and soft X-ray ranges (Schmidtke *et al.*, 2014 with personal communication from Gethyn Timothy at Harvard College Observatory).

2.2. SOLSPEC

The SOLSPEC instrument, described by Thuillier *et al.* (2009), consists of three double gratings spectrometers (which operate in the UV, Visible, and IR regions) allowing simultaneous measurements of solar spectral irradiance from 170 to 2 900 nm. The spectral resolution is a slowly varying function of the wavelengths with typical values of 1 nm at UV and visible wavelengths, and 9 nm in the IR domain. The instrument utilizes several means of on-orbit calibration. A hollow cathode lamp filled with Argon emits lines, which allow measurement of the relationship between wavelength and grating position. Deuterium lamps and tungsten ribbon lamps provide information for the instrument aging. A complete solar spectrum is measured in 11 minutes. A solar sensor provides information of the Sun's position within the field of view allowing flat-field corrections.

2.3. Other Instruments

PREMOS (*PREcision MONitoring of Solar variability*, Schmutz *et al.*, 2009) comprises several instruments presently operating onboard the *Picard* solar mission. The experiment uses filter sunphotometers and absolute radiometers to measure the spectral and total solar irradiance, respectively. The filter sunphotometers are calibrated on the absolute scale and redundant channels are periodically operated to take into account the possible aging. The spectral channels are centered at 215, 268, 535, 607, and 782 nm. For the present study of the UV SSI variability, we use the 215 nm channel, which has a spectral width of 10 nm. However, measurements in space generally require corrections to set their absolute scale,

which are not implemented here. Consequently, PREMOS data provide preliminary characterizations of the short-term variability generated by the solar rotation.

We also use data from other space instruments concurrently in operation, including

- SORCE instruments (Rottman, 2005),
- *Extreme ultraviolet Variability Experiment* (EVE, Woods *et al.*, 2012) onboard SDO,
- *Solar EUV Experiment* (SEE, Woods *et al.*, 2005) onboard TIMED.

The NASA SORCE satellite, launched in January 2003, monitors the solar spectral irradiance using three instruments, the *SOLAR STellar Irradiance Comparison Experiment* (SOLSTICE, Rottman, 2000) measuring from 115 to 320 nm, the *Solar Irradiance Monitor* (SIM, Harder *et al.*, 2005a, 2005b) operating from 200 to 2400 nm, and the *XUV Photometer System* (XPS) measuring from 0.1 nm to 34 nm and Ly α . We use SOLSTICE data version 12 available on <http://lasp.colorado.edu/lisird>.

Launched in 2002, the SEE instrument (Woods *et al.*, 2005) onboard TIMED mission measures from 0.1 to 200 nm. Within this range, the measurements in the 0.1–105 nm range are also provided by the EVE spectrometer (Woods *et al.*, 2012) onboard SDO. The measurements accuracy is 25 % or better, based on a rocket flight of the same instrument calibrated just before, and just after its retrieval.

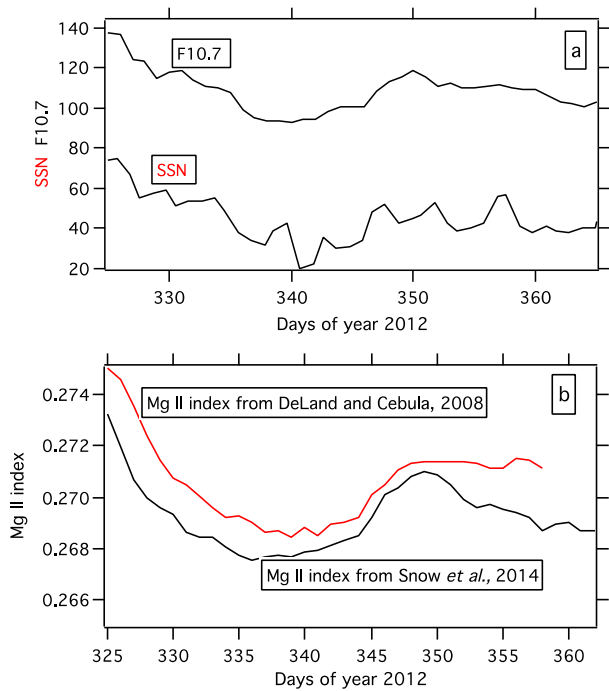
3. ISS Observing Campaign

The campaign was held between 20 November and 23 December 2012 corresponding to Carrington rotation 2131. This was a period of relatively high surface magnetic coverage, with 29 active regions listed in the NOAA catalog, including 20 appearing during the campaign *per se*. However, flaring activity remained fairly low, with 45 C-class flares across the time period, and three M-class flares observed on 27 and 28 November. The northern solar hemisphere was generally more active magnetically than its southern counterpart throughout most of CR 2131, as can be seen upon examination of SDO/HMI magnetograms (see Figure 9 further below).

3.1. ISS Attitude Change

The SolACES and SOLSPEC instruments of the SOLAR payload are mounted on the *Coarse Pointing Device* (CPD), which rotates along two axes to achieve solar pointing within nominally 5 arcminutes precision. One degree of freedom ($\pm 24^\circ$) compensates the elevation of the Sun with respect to the orbital plane of ISS. The other compensates the Sun's apparent motion along the orbit (amplitude $\pm 40^\circ$). This platform allows tracking of the Sun during 20 minutes *per* orbit, for a minimum of 10 to 14 days *per* month (designated the Solar Visibility Windows). The duration of no Sun visibility is a function of season and reaches a minimum of a few days around the solstices. Consequently, by a slight ISS attitude change, it is possible to obtain a continuous Sun visibility during one month. However, to observe a complete Sun rotation, we have to take into account the angular limitation of the CPD and to minimize the impact on the other instruments onboard the ISS during their duty cycle as well as the ISS systems (solar arrays, antenna). To achieve this opportunity, NASA/ESA have altered the attitude of the ISS by a few degrees during 11 days in order to fill the gap between two consecutive solar windows of measurements. The details of this study are given in Jacobs *et al.* (2013). This operation was managed by the Belgian User Support and Operation Center (B-USOC) ground station in charge of the SOLAR payload operations.

Figure 1 (a) $F_{10.7}$, sunspot number (SSN); (b) $Mg II$ indices by DeLand and Cebula (2008), and Snow *et al.* (2014) variation during the ISS observing campaign.



3.2. Campaign Description

Throughout the campaign, the SolACES measuring strategy was implemented, and the state of the instrument monitored (Schmidtke *et al.*, 2014). Whenever possible, a series of ionization chamber measurements *per* day and one spectrometer measurement every three or four days were carried out. From the ionization current recordings, EUV spectra are reconstructed via the modeled ionization chamber measurements.

SOLSPEC operations consist of measuring two to three solar spectra *per* day, with calibrations using the onboard lamps. In spectral domains of weak signal-to-noise ratio (*e.g.* at UV wavelengths), special commands were issued to increase the integration time of SOLSPEC's measurements. Furthermore, a special sequence of high spectral sampling measurements was undertaken in the vicinity of 280 nm to determine the $Mg II$ index variations.

3.3. Solar Activity During the Campaign

We describe solar activity during this campaign through different proxies, as shown in Figure 1. Prior to day 340 of 2012 there is general agreement between variations in sunspot number (SSN, Figure 1a) and the $Mg II$ indices (Figure 1b). However, a loss of correlation appears at certain times (day 340 and 350). Nevertheless, a minimum and a maximum are observed at day 340 and 351, respectively (Figure 1a).

The $Mg II$ time series from Snow *et al.* (2014) and DeLand and Cebula (2008) are shown in Figure 1b for days 325–365, and indicate some disagreement about the dates of maximum and minimum solar activity during the ISS campaign epoch. Since SOLSPEC also has the capability of measuring the $Mg II$ index with 0.3 % precision, we have used the method proposed by Cebula *et al.* (1992) to construct an additional $Mg II$ index for this

period. *Mg II* indices are instrument dependent due to the spectrometer spectral pass-band. This generally explains the differences in absolute values. We note that according to the SOLSPEC *Mg II* index, the day of minimum solar activity agrees with the Snow *et al.* (2014) *Mg II* time series, while the maximum agrees with DeLand's series. We also note that various proxies are sensitive to different manifestations of solar activity and therefore it is not surprising that they do not necessarily correlate strongly with each other. For example while SSN is a proxy for the coverage of the solar disk by sunspots, the *Mg II* index is a proxy for the facular coverage, and the $F_{10.7}$ index is likely sensitive to both sunspots and faculae (Tapping and DeTracey, 1990).

3.4. Measurements

3.4.1. SolACES

The variability induced by solar rotation in the EUV spectrum is around 30 %. To be reliably measured, it is necessary that instrumental stability or corrections enable temporal precision that exceeds the expected variability. Indeed, the stability of SolACES during the period of one solar rotation is less than 5 %, based on the recording of the IC currents.

In order to correct for the effect of degradation the SolACES measurements, an individual analysis of each spectrum is required. Though the gratings, parabolic mirrors, and channeltrons are individually degrading, it is not possible to trace the efficiency changes of each optical component. Instead, repeated integral re-calibration of the spectrometers is performed based on the stable ionization chamber measurements. Schmidtke *et al.* (2014) provide details as regards the data processing.

After two years of operation, the degradation of the spectrometers suggested to change the SolACES measurements strategy: the modeling of the IC current tracings allows us to reconstruct the solar EUV spectra from IC measurements, provided the transmission of the filters is known. Since there is almost no degradation with several filters and there is an easy tracing of the transmission changes for the other filters, a combination of few spectrometer measurements and regular ionization chamber measurements provide the solar SSI EUV data.

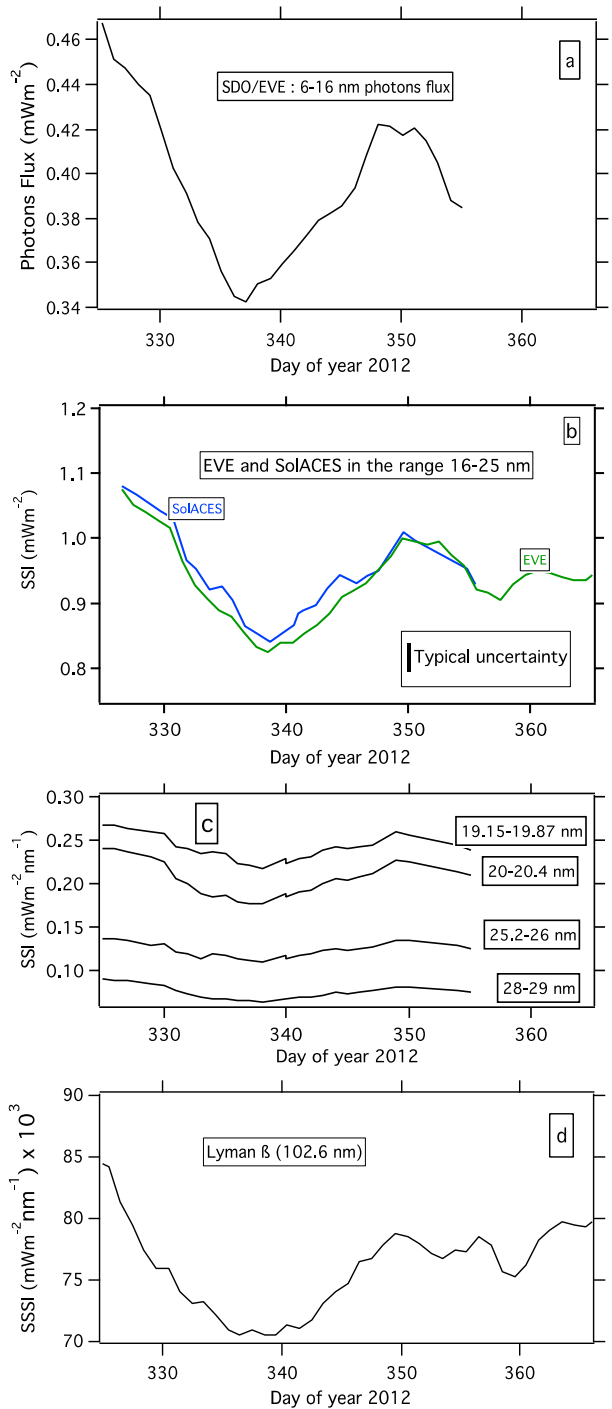
Figure 2 shows the daily mean photons flux variation from the X-ray domain measured to Ly β (102.6 nm) Figures 2a and b present the daily variation in the X-ray domain measured by SDO/EVE and the 16–25 nm range measured by SolACES and SDO-EVE. Figures 2c and d show the SolACES SSI in the EUV and the Ly β line variation during a solar rotation.

As Figure 2 illustrates, there is good agreement between SolACES and EVE in terms of absolute irradiance as well as variations as a function of time. The minimum and maximum of EUV SSI are found on day 338 and 349 of 2012, respectively. This is also observed in four selected spectral ranges gathering several lines of interest (Kenneth *et al.*, 2008), and Ly β :

- 19.15–19.8 nm (Fe XII, Fe XIII, Fe XXIV, Ca XVII)
- 20–20.4 nm (Fe XIII)
- 25.2–26 nm (Fe XIV, Fe XXII, Fe XXIV, Si X, Si XI, He II)
- 28–29 nm (Fe XIV, Fe XV, Si XI, S XII)
- Ly β (102.6 nm)

The variability is defined here as the ratio of irradiance on the day of maximum irradiance to irradiance on the day of minimum. SolACES data in the range 16–29 nm show a variability ranging from 1.19 to 1.27, which represents a weak dependence on wavelength. The variability at Ly β decreases to 1.11 as expected.

Figure 2 Shown on panels a, b, c, d, respectively, are EVE measurements in the X-ray domain, the comparisons between SolACES and EVE in the range 16–25 nm, the SolACES measurements at 19.15–19.87, 20–20.4, 25.2–26, 28–29 nm, and the irradiance at Ly β (102.6 nm).



3.4.2. SOLSPEC

As for SolACES, it is also necessary to ensure that the aging of SOLSPEC's UV channel remains negligible with respect to the expected variability generated by the solar rotation. Toward this end, the solar irradiance in the range 214–216 nm is calculated from 1 January 2010 and fitted to remove the rotation effect (around 1 %) while the aging is 13 % in two years (see in Thuillier *et al.*, 2013b, Figure 4). This corresponds to an aging of 0.15 % for the period studied here.

The SSI UV irradiance variation is displayed in Figure 3 at four wavelengths extending from 178.3 nm to 200.2 nm in spectral domains of about 1 nm. The instrument operation has allowed up to three spectra per day. The average was calculated and displayed in Figure 3, nevertheless the data are noisy at these wavelengths. The polynomial fit was used to better define the days of maximum and minimum.

Maximum and minimum SSI occur on the same days in the different time series and are nearly in phase with the EUV irradiance variations shown in Figure 2. The maximum to minimum SSI ratio measured by SOLSPEC is 1.016. For this article, we were not ready to make the aging correction needed after five years in orbit. For consistency with the other spectra in absolute scale (including PREMOS), we have scaled SOLSPEC in relative scale to SOLSTICE-SORCE SSI at day 347.

3.4.3. Other Spectral Irradiance Observations

Figure 4 shows the SSI from the 215 nm channel measured by PREMOS.

PREMOS data at 215 nm show similar variations in phase with those observed by SOLSPEC (Figure 3). The SSI maximum to minimum ratio is equal to 1.006.

SOLSTICE provides data at 215.5 nm, however, only available from day 343. Only the maximum SSI is available and found on day 350 (a plot is shown in Figure 8).

As a preliminary conclusion, the simultaneous maximum and minimum SSI occurrence is then observed from the X-rays to UV.

4. Models of Solar Spectral Irradiance EUV Variability

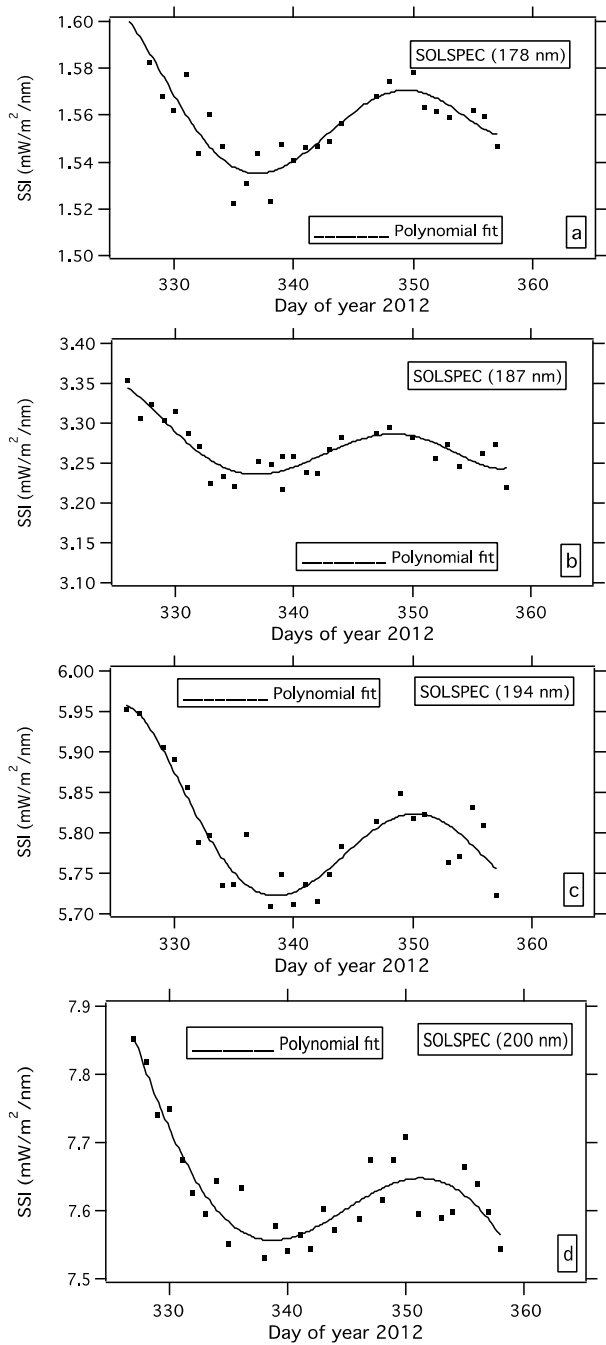
SolACES measurements during the ISS campaign are compared with two different models of solar EUV irradiance variability; one model (SOLMOD) utilizes physical descriptions of the solar atmosphere in quiet and active regions to estimate the contributions of active region features to EUV irradiance changes while the second model (NRLSSI) is constructed from wavelength-dependent statistical relationships between the solar EUV irradiance measured by TIMED/SEE from 2002 to 2014 with solar activity proxies (Lean *et al.*, 2011).

4.1. SSI Reconstruction of the EUV Based on SOLMOD

4.1.1. AIA Image Segmentation

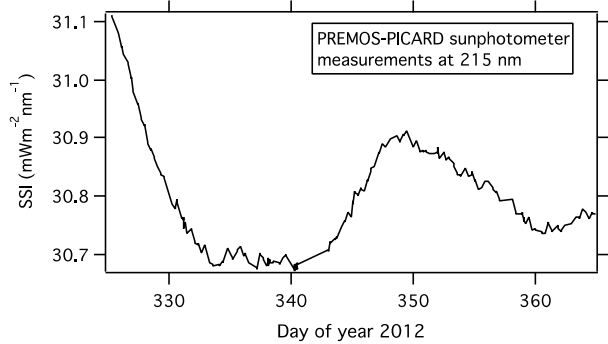
For input to SOLMOD, the area coverage of the coronal features is determined from images of the solar corona. In the current study, images obtained with the *Atmospheric Imaging Assembly* (AIA, Lemen *et al.*, 2012) onboard SDO are employed. The feature identification is carried out with the Spatial Possibilistic Clustering Algorithm tool (Verbeeck *et al.*, 2013, SPoCA), a suite of algorithms designed to perform the pixel-intensity based segmentation

Figure 3 SOLSPEC variations of SSI at 178.3, 187.1, 193.7, and 200.2 nm are shown in panels a, b, c, d, respectively. The solid line is a polynomial fit.



of EUV images. Following the approach described in Haberreiter *et al.* (2014), the area covered by six different solar activity features, *i.e.* Coronal Holes (CH), Quiet Sun 1 (QS₁),

Figure 4 PREMOS measurements at 215 nm.



Quiet Sun 2 (QS₂), Active Region 1 (AR₁), Active Region 2 (AR₂), and Active Region 3 (AR₃), is determined for concentric rings r_i from disk center to 1.3 solar radii.

4.1.2. EUV Reconstruction

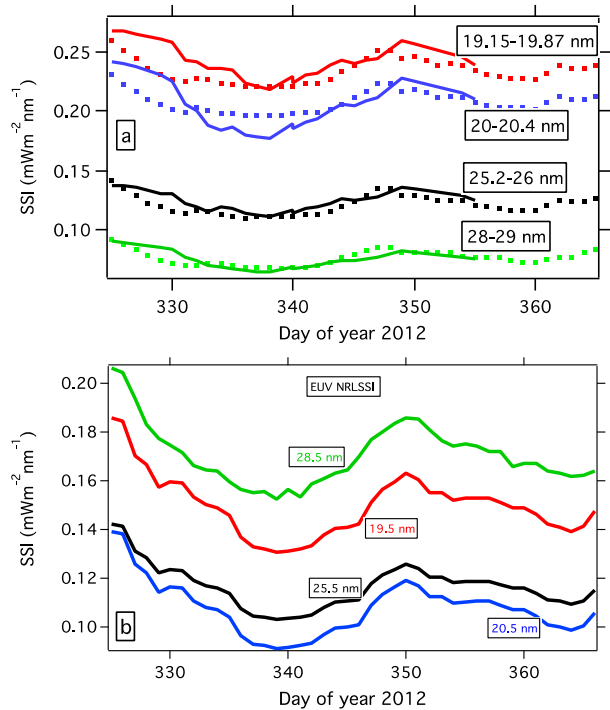
We use the SOLMOD code, which is a variant of the Solar Radiation Physical Modeling code (see Fontenla, Balasubramaniam, and Harder, 2007; Fontenla *et al.*, 2014 and references therein) to calculate synthetic EUV spectra for each coronal feature. The description of SOLMOD is given in Haberiter (2011). We employ the coronal atmosphere structures as described by Haberiter (2012) for the five different components of the corona: QS₁, QS₂, AR₁, AR₂, and AR₃. The dark CHs are considered as having a contrast of 0.5 with respect to QS₁. The time-dependent EUV irradiance is then calculated as the sum of the synthetic spectra weighted by the respective area coverage.

4.2. SSI Reconstruction of the EUV Based on NRLSSI

The Naval Research Laboratory Solar Spectral Irradiance (NRLSSI) variability model calculates the Sun's extreme ultraviolet (EUV) irradiance in 1 nm bins from 0 to 120 nm using parameters derived from multiple regression of the *Mg II* and $F_{10.7}$ solar activity indices with irradiance observations made by the *Solar EUV Experiment* (SEE) on the *Thermosphere Ionosphere Mesosphere Energetic and Dynamics* (TIMED) spacecraft since 2002 (Woods *et al.*, 2005). As described by Lean *et al.* (2011), a model version designated 3C empirically relates the SEE observations in each 1 nm wavelength band to the daily and (time-centered) 81-day smoothed *Mg II* and $F_{10.7}$ indices. The 2C version of the model also utilizes wavelength-dependent combinations of the *Mg II* and $F_{10.7}$ indices of solar activity, but to reproduce only the observed rotational modulation; solar cycle variations are determined by the long-term variations in the two indices rather than by the SEE observations directly.

As originally formulated (Lean *et al.*, 2011), NRLSSI used the SEE Version 10 database from 2002 to 2010 (the descending phase of Solar Cycle 23) to determine the model's wavelength-dependent scalings of the *Mg II* and $F_{10.7}$ indices, using the original NOAA SBUV *Mg II* composite compiled by Viereck *et al.* (2004), extended with an *Mg II* index determined from SORCE-SOLSTICE measurements (Snow *et al.*, 2005). For comparison with the SolACES observations, the NRLSSI model was reformulated (and designated NRLSSI2), using the SEE Version 11 database from 2002 to 2014 and the GOME *Mg II* index (Skupin *et al.*, 2004). Used here for comparison with the SolACES observations are the

Figure 5 Panel (a) shows the SOLMOD (dotted lines), and SolACES measurements (solid lines) in four spectral intervals. Panel (b) shows the NRLSSI reconstructions in bins close to those of SolACES.



solar EUV irradiance variations specified by version 3C of the NRLSSI2 model, although on solar rotational time scales the 3C and 2C models are essentially equivalent (see Lean *et al.*, 2011, Figure 7).

4.3. Comparison Between SolACES Measurements and Models in the EUV Range

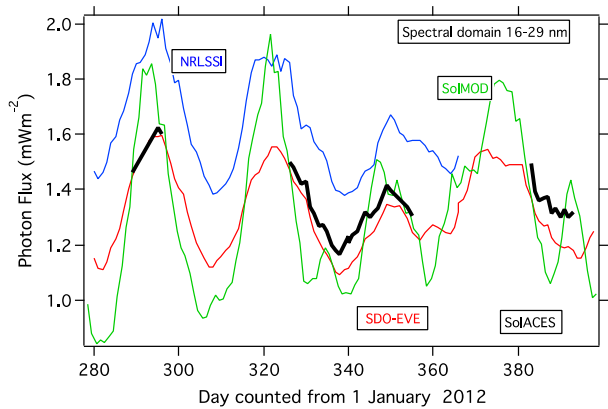
Figure 5a shows the EUV reconstruction for the five spectral intervals 19.15–19.87 nm, 20–20.4 nm, 25.2–26 nm, 28–29 nm, measured with SolACES and modeled with SOLMOD. The absolute level of the EUV reconstruction has been adjusted to the irradiance level of SolACES. This implies a correction of the minimum level of 90 % for 19.15–19.87 nm, 75 % for 20–20.4 nm, 40 % for 25.2–26 nm, 30 % for 28–29 nm, and 30 % for the 16–25 nm interval. SOLMOD predicts the SSI and days of maximum and minimum Irradiance from which the SSI variability is calculated. These results are in agreement with SolACES, but not the absolute values. In order to show the agreement of the days of extrema with SolACES using a the figure, a value (wavelength dependent) was added to the minimum level (given in % of the minimum). The text is correct. Figure 5a only aims to show the agreement between SOLMOD and SolACES concerning the days of extrema in order to present all data (SolACES and SOLMOD) in the same Figure 5a. The correction for the two first intervals is rather high. Updating the atomic data used in SOLMOD is expected to improve the agreement with the observations. The irradiance variability as modeled with SOLMOD is wavelength dependent and varies between a factor of 1.17 to 1.52. The SolACES measurements indicate that the irradiance variability varies between a factor of 1.19 to 1.27 with a mean of 1.23.

Figure 5b presents the NRLSSI in four spectral domains close to the domains observed by SolACES. NRLSSI data are available in 1 nm bins, so precise comparisons with SolACES

Table 1 EUV predictions and measurements comparison in the four spectral domains measured by SoLACES, SOLMOD, and NRLSSI. Measurements are indicated by italics.

<i>Instruments/Reconstruction</i>	Maximum to minimum ratio	Day of SSI minimum	Day of SSI maximum
<i>SolACES</i>	<i>1.19 to 1.27</i>	<i>339</i>	<i>350</i>
SOLMOD	1.17 to 1.52	331 and 340	348
NRLSSI	1.22 to 1.30	339	350

Figure 6 Integrated intensity of the spectral solar irradiance from 16 nm to 29 nm is shown for SDO/EVE, SOLAR/SoLACES, NRLSSI, and SOLMOD in mW m^{-2} for four solar rotations. The range of absolute uncertainty of both measured data sets is 10 %.



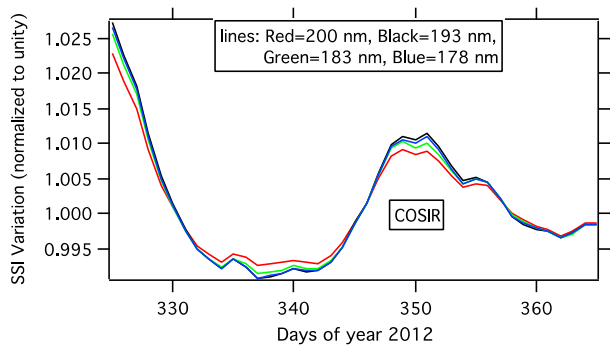
bins are not possible. Nevertheless, the day of maximum and minimum SSI are those of SoLACES. NRLSSI variability is slightly wavelength dependent as SoLACES and SOLMOD ranging from 1.22 to 1.30, however, closer to measurements than SOLMOD (Table 1).

Table 1 presents the variability and the phase of the maximum and minimum SSI measured by SoLACES and predicted by the models. The closest predictions with respect to SoLACES are provided by NRLSSI.

A similar comparison between SoLACES and SDO-EVE is shown in Figure 6 over four solar rotations including the period of the present study. The agreement between the two measured data sets is within 10 %.

Figure 6 also shows the NRLSSI variability in good agreement with the observations. However, its absolute values are about 25 % greater than the measurements, the reason for this being that the NRLSSI-EUV model is based on the TIMED-SEE data. Thus the differences in absolute values presumably reflect differences in the absolute calibrations of the SEE and EVE instruments. The SOLMOD reconstruction has been shifted by $+0.1 \text{ mW/m}^2$. Overall, the SOLMOD reconstruction shows a higher rotational variation than the observation. The reason for this is that for the AIA image segmentation, the theoretical contrast values calculated from the SOLMOD atmosphere models are employed. Due to currently uncorrected straylight in the AIA observation, the observed contrast of the coronal features is lower than the theoretical contrast we apply. Therefore, generally the variability of the reconstruction is overestimated. In particular, this explains the peak around day 386, for which an overestimated contribution of feature AR₁ is responsible. The reconstruction taking the AIA straylight correction into account is currently being worked on.

Figure 7 Daily variation of SSI as a function of wavelength calculated by COSIR and normalized to day 365.



5. Models of Solar Spectral Irradiance UV Variability

A recent analysis of five SSI reconstructions operating above Ly α , has been published by Thuillier *et al.* (2013a) who compared the following models:

- MOCASSIM (Bolduc *et al.*, 2012).
- MGNM (Thuillier *et al.*, 2012).
- NRLSSI (Lean, 2000).
- SATIRE (Krivova, Solanki, and Unruh, 2011).
- SEA (Shapiro *et al.*, 2011).

These models use as inputs different proxies and spectral intensity contrasts, either theoretical or measured. The analysis mentioned above summarizes their key principles and properties, which are not repeated here. Rather, we compare their predictions on the solar rotation time scale with measurements carried out during the ISS observational campaign.

While the Shapiro *et al.* (2011) model only provides annual values of the solar irradiance, the new model COSIR (CODE of Solar Irradiance Reconstruction) allows calculation of solar irradiance with daily resolution. COSIR, as introduced in Cessateur *et al.* (2014), is a five-component reconstruction of solar spectral irradiance, which treats separately the contribution from the quiet Sun, sunspots (umbra and penumbra), active network and plages. The filling factors for COSIR have been provided by Yeo *et al.* (2014) who used full-disc magnetograms and intensity images by the *Helioseismic and Magnetic Imager* (HMI, Schou *et al.*, 2012) onboard SDO. These filling factors are then convolved with the synthetic spectra calculated with the COSI code by Haberleiter, Schmutz, and Hubeny (2008) and Shapiro *et al.* (2010). Cessateur *et al.* (2014) give a detailed comparison of the solar irradiance variability as calculated by COSIR and measured by PREMOS, which will also be shown below (Figure 9) with other SSI predictions.

5.1. Dates of Maximum and Minimum Irradiance

In the UV domain, the reconstructions exhibit spectral variability that are almost independent of wavelength. This is illustrated for COSIR in Figure 7, for wavelengths measured by SOLSPEC.

There is a very small variation of the shape. We have verified this property for the four other reconstructions in the same spectral domain. This property allows us to choose a wavelength for comparison of the five reconstructions variability. We have chosen 215 nm, which was observed by PREMOS.

Figure 8 Shown are from the top to the bottom COSIR, MGNM (using the two $Mg II$ series, one from DeLand and Cebula (2008), another from Snow *et al.* (2014), MOCASSIM, NRLSSI, SATIRE reconstructions at 215 nm, and SOLSTICE/SORCE data. As PREMOS data are not in the absolute scale, an arbitrary adjustment with a coefficient 1.09 is applied to scale the observations to within the range of the figure.

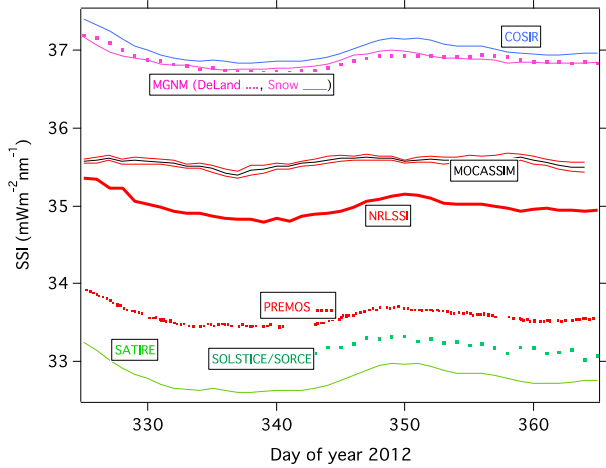
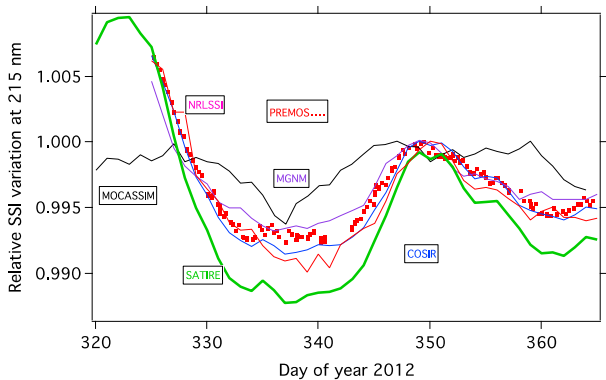


Figure 9 The relative SSI variation shows the agreement among the SSI simulations in terms of days of minima and maxima, and relative variation.



5.2. Models and PREMOS Data at 215 nm Comparison

Figures 8, 9, 10 display PREMOS measurements and several models.

Figure 8 compares the five reconstructions of solar UV irradiance at 215 nm. Absolute SSI values show large variations from one reconstruction to the other, but the days of maximum and minimum SSI are in close agreement within one day. The MOCASSIM model stands apart from the other reconstructions in that it does not use daily images or indices. Instead, the surface coverage of magnetic structures is generated by a surface magnetic flux evolution model driven by active region emergences. Because backside and near-limb emergences are not observed, a stochastic procedure injects additional active regions at the same rate as observed emergences, in order to correctly capture the cycle amplitude. This implies that over any given month, up to two thirds of emergences occur at the wrong longitude or day (see Section 2.1 in Crouch *et al.* (2008) for more details of this procedure). It is therefore not surprising that MOCASSIM fails to properly reproduce observed spectral irradiance variations on daily to monthly timescales.

Figure 9 presents the variation in relative unit, together with PREMOS data, and illustrates the agreement in the temporal variation of the solar irradiance. The three closest reconstructions to PREMOS are NRLSSI, COSIR, and MGNM.

Figure 10 Shown are the PREMOS data, and the two MGNM reconstructions, using the DeLand and Cebula (2008) and Snow *et al.* (2014) *Mg II* index series. The row of images at the bottom are four magnetograms from HMI/SDO illustrating the coverage of the solar disk with magnetic features as a function of time. As PREMOS data are not in the absolute scale, an arbitrary adjustment is applied to scale the reconstructions to within the range of the figure.

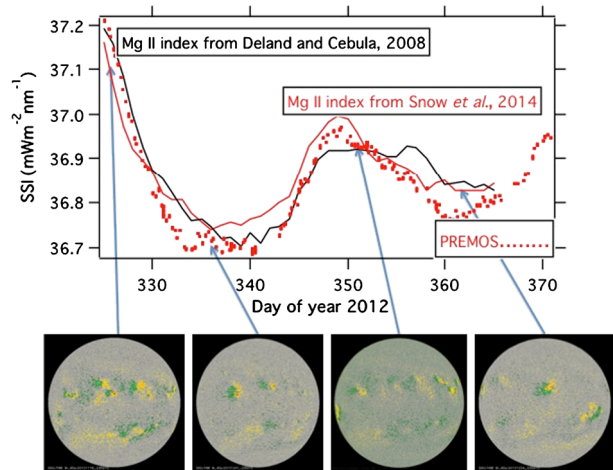


Table 2 SSI variability and SSI absolute value predicted by five reconstructions compared to measurements by PREMOS and SOLSTICE at 215 nm.

Instruments/ Reconstructions	Maximum to minimum ratio	Maximum SSI ($\text{mW m}^{-2} \text{nm}^{-1}$)	Day of SSI minimum	Day of SSI maximum
PREMOS	1.006	NA	338	350
SOLSTICE/SORCE	1.010	33.3	338	349
COSIR	1.008	37.15	340	350
MGNM (<i>Mg II</i> index)	1.006	36.99	340	350
MOCASSIM	1.007	35.5	338	350
NRLSSI	1.008	35.14	338	350
SATIRE	1.013	32.97	339	350

Figure 10 compares the variations predicted by the two MGNM reconstructions: that based on Snow *et al.*'s *Mg II* index provides closer predictions than does DeLand's index when compared to PREMOS variation. Interestingly, the MGNM empirical model shows slightly less variability than the PREMOS measurements indicate (in particular, MGNM gives higher irradiance values around day 360). This is caused by the fact that the *Mg II* index is mainly sensitive to faculae and is basically unaffected by the sunspots so that Figures 8, 9, 10 suggest that there is a spot contribution to the 215 nm SSI (see Cessateur *et al.*, 2014).

The five models are in phase as the values in Table 2 show. Dates of minimum and maximum agree within one day. Furthermore, the dates of maximum and minimum SSI predicted by these models are not wavelength dependent *per* constructions. We note that the smallest irradiance is predicted by SATIRE to about $3 \text{ mW m}^{-2} \text{ nm}^{-1}$ lower than the mean of the four other predicted irradiance values, however, very close to SOLSTICE measurements.

Figure 8 also shows that the irradiance time variations using the two *Mg II* indices generate wavelength-dependent differences of the order of $0.1 \text{ mW m}^{-2} \text{ nm}^{-1}$. In the analysis of different SSI reconstructions (Thuillier *et al.*, 2013a) one has discussed their accuracy. Given the time-dependent accuracy of each proxy time series, their different combinations utilized in each reconstruction, together with the uncertainty of the spectra used to provide the mod-

els' absolute scales, it was concluded that quoting the accuracy of a given reconstruction was not possible as yet, and that the best way to estimate its accuracy was the comparison with other models and measured spectra. Applying this strategy here, the different amplitudes of the maximum are consistent within 6 %, around $35 \text{ mW m}^{-2} \text{ nm}^{-1}$ (Table 2).

COSIR, MGNM (Snow's series), NRLSSI, and SATIRE's SSI at 215 nm after the maximum at day 350 are decreasing with time at a rate larger than predicted by MOCASSIM. Maximum irradiance is consistently found at day 350, while a lesser agreement is found for the day of minimum irradiance.

6. Conclusions

As part of a special ISS solar observing campaign of Carrington rotation # 2131 (days 325 – 360 of 2012), we have gathered several data sets of solar spectral irradiance observations at EUV and UV wavelengths. The movement of the active regions across the instrument field of view generates a solar irradiance modulation, as a function of day which is evident in all the available data. We find that for wavelengths from 16 to 215 nm the maximum and minimum irradiance occur nearly in phase (within a day). Furthermore the mean irradiance ratio is 1.23 in the EUV range. In the UV spectrum, the dates of maximum and minimum are the same as in the EUV domain, however, the irradiance ratio is significantly lower and found to be around 1.01.

Measurements have been compared with a variety of different models, all of which are based on solar activity features (SSN, *Mg II* index, etc.):

For the EUV, the SOLMOD reconstruction was employed, predicting days of maximum close to the measurements but not in close agreement with the observed minimum. Furthermore, the irradiance ratio is found between 1.17 to 1.52 wavelength dependent, while measurements provide less (1.19 to 1.27 also wavelength dependent). However, the absolute level of the simulated spectral EUV irradiance needs to be adjusted by 30 % to 90 % to agree with the measurements. NRLSSI EUV predicts an amplitude of the variability as well as a phase of the maximum and minimum SSI in close agreement with SolACES. This result is also true over the four available rotations for which some SolACES data are available. However, its absolute values are about 25 % greater than the measurements, likely due to the use of the SEE/TIMED data.

For the UV spectral irradiance, five models were compared with the ISS-based observations and all provided consistent predictions in terms of days of maximum and minimum irradiance with an irradiance ratio close to the measurements (≈ 1 %) and nearly wavelength independent. Using DeLand's and Snow's *Mg II* time series as input to the MGNM reconstruction yields wavelength-dependent differences reaching $0.1 \text{ mW m}^{-2} \text{ nm}^{-1}$ at 215 nm. Among the five reconstructions COSIR, and MGNM's irradiance remain within $0.2 \text{ mW m}^{-2} \text{ nm}^{-1}$ around $37 \text{ mW m}^{-2} \text{ nm}^{-1}$; MOCASSIM and NRLSSI are within $0.3 \text{ mW m}^{-2} \text{ nm}^{-1}$ around $35.5 \text{ mW m}^{-2} \text{ nm}^{-1}$, while SATIRE is the lowest at $32.7 \text{ mW m}^{-2} \text{ nm}^{-1}$, however, close to the SOLSTICE measurements.

Detailed comparisons of the calculated short-term variability from different models with observations, such as we report here, are important for validating the physics of these models; an example has been shown with the specific role of the sunspots even in the UV.

Acknowledgements The SOLSPEC and SolACES investigations are supported by the Centre National d'Etudes Spatiales (France), the Centre National de la Recherche Scientifique (France), the Federal Office for Scientific, Technical and Cultural Affairs (Belgium), and the Bundesministerium für Forschung und Technologie (Germany). The participating institutes are the Service d'Aéronomie du CNRS, now LATMOS,

the Institut d'Aéronomie Spatiale de Belgique, the Fraunhofer Institute for Physical Measuring Technique (Freiburg), and the Landessternwarte of Heidelberg. The SOLSPEC and SolACES absolute calibrations have been carried out with the blackbody BB3200g from the Physikalisch-Technische Bundesanstalt (PTB, Braunschweig, Germany), and cross-calibrated at BESSY II (PTB, Berlin, Germany), respectively. SOLAR constitutes an external payload of the ESA COLUMBUS laboratory placed onboard the *International Space Station*. The SOLAR operations are conducted by the Belgium User Support Operations Center (B-USOC) via the COLUMBUS Control Center of DLR (Oberpfaffenhofen, Germany). SolACES has been developed by the Fraunhofer IPM. EADS Astrium Friedrichshafen supported the institute in performing the qualification and documentation. The project was sponsored by DLR, ESA, and the Fraunhofer Gesellschaft. A. I. Shapiro is supported by the Swiss National Science Foundation under grant CRSI122-130642 (FUPSOL) and 100020 140573. C. Bolduc and P. Charbonneau are supported by a team grant and a doctoral fellowship from the Fond Québécois pour la Recherche en Nature et Technologie. We are happy to thank J. Harder and, M. Snow and M. DeLand for providing the SIM data and *Mg II* index, respectively, and B-USOC for providing the raw SOLSPEC data used in this study. The research leading to these results has received funding from the European Community's Seventh Framework Programme (FP7 2012) under grant agreement No. 313188 (SOLID). G. Cessateur is supported by the FP7 programme (eHeroes, No. 284461). J. Lean acknowledges NASA support.

Finally, we thank the referee for his valuable report.

References

- Anet, J.G., Muthers, S., Rozanov, E.V., Raible, C.C., Stenke, A., Shapiro, A.I., Bronnimann, S., Arfeuille, F., Bruignara, Y., Beer, J., Steinhilber, F., Schmutz, W., Peter, T.: 2013, *Clim. Past Discuss.* **9**, 6179. DOI.
- Bolduc, C., Charbonneau, P., Dumoulin, V., Bourqui, M.S., Crouch, A.D.: 2012, *Solar Phys.* **279**, 383. DOI.
- Bovensmann, H., Burrows, J.P., Buchwitz, M., Frerick, J., Noel, S., Rozanof, V.V., Chance, K.V., Goede, A.P.H.: 1999, *J. Atmos. Sci.* **56**, 127. DOI.
- Brueckner, G.E., Edlow, K.L., Floyd, L.E., Lean, J.L., VanHoosier, M.E.: 1993, *J. Geophys. Res.* **98**, 10695. DOI.
- Cebula, R.P., DeLand, M.T., Schlesinger, B.M.: 1992, *J. Geophys. Res.* **97**(D11), 11613. DOI.
- Cessateur, G., Shapiro, A.I., Yeo, K.L., Krivova, N.A., Tagirov, R., Adams, W., Schmutz, W.: 2014, *Astron. Astrophys.*, submitted.
- Crouch, A.D., Charbonneau, P., Beaubien, G., Paquin-Ricard, D.: 2008, *Astrophys. J.* **677**, 723. DOI.
- DeLand, M.T., Cebula, R.P.: 2008, *J. Geophys. Res.* **113**, A11103. DOI.
- Dominique, M., Hochedez, J.-F., Schmutz, W., Dammash, I.E., Shapiro, A.I., Kretzchmar, M., Zhukov, A.N., Gillotay, D., Stockman, Y., Benmoussa, A.: 2013, *Solar Phys.* **286**, 21. DOI.
- Fontenla, J.M., Balasubramaniam, K.S., Harder, J.: 2007, *Astrophys. J.* **667**, 1243. DOI.
- Fontenla, J.M., Landi, E., Snow, M., Woods, T.: 2014, *Solar Phys.* **289**, 515. DOI.
- Haberreiter, M.: 2011, *Solar Phys.* **274**, 473. DOI.
- Haberreiter, M.: 2012, *Proc. IAU Symp.* **286**, 97. DOI.
- Haberreiter, M., Schmutz, W., Hubeny, I.: 2008, *Astron. Astrophys.* **492**, 833. DOI.
- Haberreiter, M., Dellouille, V., Mampaey, B., Verneck, C., Del Zanna, G., Wieman, S.: 2014, *J. Space Weather Space Clim.* under minor revision.
- Haigh, J.D., Winning, A., Toumi, R., Harder, J.W.: 2010, *Nature* **467**, 696. DOI.
- Harder, J.W., Fontenla, J., Lawrence, G., Woods, T.N., Rottman, G.: 2005a, *Solar Phys.* **230**(1–2), 169. DOI.
- Harder, J.W., Lawrence, G., Fontenla, J., Rottman, G., Woods, T.N.: 2005b, *Solar Phys.* **230**(1–2), 141. DOI.
- Harder, J.W., Thuillier, G., Richard, E.C., Brown, S.W., Lykke, K.R., Snow, M., McClintock, W.E., Fontenla, J.M., Woods, T.N., Pilewskie, P.: 2010, *Solar Phys.* **263**, 3. DOI.
- Jacobs, C., Van Hoof, D., Wislez, J.M., Sela, A., Michel, A., This, N., et al.: 2013 BUSOC-ISS SOLAR Bridging Report, IAC-13-B3.4-B6.5.2.
- Kenneth, J.H.Ph., Feldman, U., Landi, E.: 2008, *Ultraviolet and X-Ray Spectroscopy of the Solar Atmosphere, Cambridge Astrophysics Series* **44**.
- Krivova, N.A., Solanki, S.K., Unruh, Y.C.: 2011, *J. Atmos. Solar-Terr. Phys.* **73**, 223. DOI.
- Lean, J.: 2000, *Geophys. Res. Lett.* **27**, 2425. DOI.
- Lean, J.L., DeLand, M.T.: 2012, *J. Climate* **25**, 2556. DOI.
- Lean, J.L., Woods, T.N., Eparvier, F., Meier, R.R., Strickland, D.J.: 2011, *J. Geophys. Res.* **116**, A01102. DOI.
- Lemen, J.R., Title, A.M., Akin, D.J., Boerner, P.F., Chou, C., Drake, J.F., Duncan, D.W., Edwards, C.G., Friedlaender, F.M., Heyman, G.F., Hurlburt, N.E., Katz, N.L., Kushner, G.D., Levay, M., Lindgren, R.W., Mathur, D.P., McFeaters, E.L., Mitchell, S., Rehse, R.A., Schrijver, C.J., Springer, L.A., Stern,

- R.A., Tarbell, T.D., Wuelser, J.-P., Wolfson, C.J., Yanari, C., Bookbinder, J.A., Cheimets, P.N., Caldwell, D., Deluca, E.E., Gates, R., Golub, L., Park, S., Podgorski, W.A., Gummin, M.A., Smith, P., Auker, G., Jerram, P., Pool, P., Soufli, R., Windt, D.L., Beardsley, S., Clapp, M., Lang, J., Waltham, N.: 2012, *Solar Phys.* **275**, 17. DOI.
- McClintock, W.E., Rottman, G.J., Woods, T.N.: 2005, *Solar Phys.* **230**, 225. DOI.
- Meehl, G.A., Tebaldi, C., Walton, G., Easterling, D., McDaniel, L.: 2009, *Geophys. Res. Lett.* **36**(23), L23701. DOI.
- Rottman, G.: 2000, *Space Sci. Rev.* **94**(1/2), 83. DOI.
- Rottman, G.J.: 2005, *Solar Phys.* **230**, 7. DOI.
- Rottman, G.J., Woods, T.N., Sparr, T.P.: 1993, *J. Geophys. Res.* **98**, 10667. DOI.
- Schmidt, G.A., Jungclaus, J.H., Ammann, C.M., Bard, E., Braconnot, P., Crowley, T.J., et al.: 2011, *Geosci. Model Dev.* **4**, 33. DOI.
- Schmidtke, G., Fröhlich, C., Thuillier, G.: 2006b, *Adv. Space Res.* **37**(2), 255. DOI.
- Schmidtke, G., Brunner, R., Eberhard, D., Halford, B., Klocke, U., Knothe, M., Konz, W., Riedel, W.J., Wolf, H.: 2006a, *Adv. Space Res.* **37**, 273. DOI.
- Schmidtke, G., Nikutowski, B., Jacobi, Ch., Brunner, R., Erhardt, Ch., Knecht, S., Scherle, J., Schlagenhauf, J.: 2014, *Solar Phys.* **289**, 1863. DOI.
- Schmutz, W., Fehlmann, A., Hüsen, G., Meindl, P., Winkler, R., Thuillier, G., et al.: 2009, *Metrologia* **46**, S202. DOI.
- Schou, J., Scherrer, P.H., Bush, R.I., Wachter, R., Couvidat, S., Rabello-Soares, M.C., et al.: 2012, *Solar Phys.* **275**, 229. DOI.
- Shapiro, A.I., Schmutz, W., Schoell, M., Haberreiter, M., Rozanov, E.: 2010, *Astron. Astrophys.* **517**, A48. DOI.
- Shapiro, A.V., Rozanov, E., Egorova, T., Shapiro, A.I., Peter, T., Schmutz, W.: 2011, *J. Atmos. Solar-Terr. Phys.* **73**, 348. DOI.
- Skupin, J., Weber, M., Bovensmann, H., Burrows, J.P.: 2004, The Mg II solar activity proxy indicator derived from GOME and SCIAMACHY. In: *Proceedings of the ENVISAT & ERS Symposium (SP-572)*, ESA Publications Division.
- Snow, M., McClintock, W.E., Woods, T.N., White, O.R., Harder, J.W., Rottman, G.: 2005, *Solar Phys.* **230**, 325. DOI.
- Snow, M., Weber, M., Machol, J., Viereck, R., Richard, E.: 2014, *J. Space Weather Space Clim.* **4**, A04. DOI.
- Tapping, K.F., DeTracey, B.: 1990, *Solar Phys.* **127**, 321. DOI.
- Thuillier, G., Foujols, T., Bolsée, D., Gillotay, D., Hersé, M., Peetermans, W., Decuyper, W., Mandel, H., Sperfeld, P., Pape, S., Taubert, D.R., Hartmann, J.: 2009, *Solar Phys.* **257**, 185. DOI.
- Thuillier, G., DeLand, M., Shapiro, A., Schmutz, W., Bolsée, D., Melo, S.M.L.: 2012, *Solar Phys.* **277**, 245. DOI.
- Thuillier, G., Bolsée, D., Schmidtke, G., Foujols, Th., Nikutowski, B., Brunner, R., Erhardt, Ch., Shapiro, A.V., Schmutz, W., Hersé, M., Gillotay, D., Mandel, H., Petermanns, W., Decuyper, W.: 2013b, *Solar Phys.* **289**, 1931. DOI.
- Thuillier, G., Melo, S.M.L., Lean, J., Krivova, N., Bolduc, C., Charbonneau, P., Shapiro, A.V., Schmutz, W., Bolsée, D.: 2013a, *Solar Phys.* **289**, 1115. DOI.
- Verbeeck, C., Higgins, P.A., Colak, T., Watson, F.T., Delouille, V., Mampaey, B., Qahwaji, R.: 2013, *Solar Phys.* **283**, 67. DOI.
- Viereck, R.A., Floyd, L.E., Crane, P.C., Woods, T.N., Knapp, B.G., Rottman, G., Weber, M., Puga, L.C.: 2004, *Space Weather* **2**, S10005. DOI.
- Woods, T.N., Eparvier, F.G., Bayley, S.M., Chamberlain, P.C., Lean, J., Rottman, G.J., Solomon, S.C., Tobiska, W.K., Woodraska, D.L.: 2005, *J. Geophys. Res.* **110**, AO1312. DOI.
- Woods, T.N., Eparvier, F.G., Hock, R., Jones, A.R., Woodraska, D., Judge, D., Didkovsky, L., Lean, J., Mariska, J., Warren, H., McMullin, D., Chamberlin, P., Berthiaume, G., Bailey, S., Fuller-Rowell, T., Sojka, J., Tobiska, W.K., Viereck, R.: 2012, *Solar Phys.* **275**, 115. DOI.
- Yeo, K.L., Krivova, N.A., Solanki, S.K., Glassmeier, K.H.: 2014, *Astron. Astrophys.*, in press. DOI.